



PROCUREMENT EXECUTIVE, MINISTRY OF DEFENCE

Aeronautical Research Council  
Reports and Memoranda

PREDICTION OF CRACK GROWTH  
IN DAMAGE-TOLERANT DESIGN-  
A BASIC PARAMETRIC STUDY

by

Vera J. Pike

W.T. Kirkby

Structures Department, RAE Farnborough, Hants

LIBRARY  
ROYAL AIRCRAFT ESTABLISHMENT  
BEDFORDS.

London: Her Majesty's Stationery Office

1978

PRICE £4 NET

PREDICTION OF CRACK GROWTH IN DAMAGE-TOLERANT DESIGN -  
A BASIC PARAMETRIC STUDY

By Vera J. Pike and W. T. Kirkby

Structures Department, RAE, Farnborough, Hants

---

Reports and Memoranda No.3822\*

February 1977

---

SUMMARY

A study has been undertaken to obtain some experience of the difficulties likely to arise in predicting crack behaviour when implementing the damage-tolerant design philosophy and to obtain an indication of the influence of some of the design parameters involved on life to failure. The study was centred on the growth of a corner-crack from a hole in an infinite plate, remotely loaded. The parameters considered included hole diameter, initial crack length and the severity of the spectrum of applied loads. Predictions of life were made for five different aluminium alloys. The study highlighted difficulties associated both with the analytical method and with shortcomings in available materials data. The results of the life predictions showed that, as would be expected, the predominant parameter was spectrum severity. However, variation of the other parameters within a reasonable range also resulted in significant changes in life (typically in the region of 5:1), the influence of change of material being only slightly greater.

---

\* Replaces RAE Technical Report 77026 - ARC 37438

LIST OF CONTENTS

	<u>Page</u>
1 INTRODUCTION	3
2 FAIL-SAFE AND DAMAGE-TOLERANT DESIGN - AN OUTLINE	4
3 THE PREDICTIONS	6
3.1 The model	7
3.2 The stress spectra	7
3.3 Materials	8
3.4 Method of prediction	9
4 SOME AREAS OF DIFFICULTY IN THE PREDICTIONS	9
4.1 Analytical difficulties	10
4.2 Shortcomings in materials data	11
5 PRESENTATION AND DISCUSSION OF RESULTS	12
5.1 General	12
5.2 Effect of spectrum severity on endurance	14
5.3 Influence of hole diameter and initial crack length on endurance	15
6 CONCLUDING OBSERVATIONS	15
Appendix A Derivation of stress intensity factors	19
Appendix B Description of prediction method	21
Tables 1 to 4	24
References	27
Illustrations	Figures 1-9
Detachable abstract cards	-

## 1 INTRODUCTION

The problem of ensuring satisfactory fatigue performance of an aircraft structure continues to be a major consideration in design. Comparatively recently a new design approach has been put forward which is referred to as the 'damage-tolerant'\* design philosophy<sup>1</sup> and it has excited considerable interest because of the potential contribution to increased structural safety and reliability. The work which forms the subject of this Report had two main objectives. The first was to obtain some experience of the nature of the detailed problems likely to be encountered by a designer in predicting crack behaviour when implementing the damage-tolerant design philosophy and the second was to obtain an indication of the influence on life to failure of some of the design parameters involved.

The damage-tolerant design philosophy follows, chronologically, the 'safe-life' design philosophy<sup>2</sup> which was evolved in the years immediately following World War II and the 'fail-safe'\* design approach<sup>2</sup>, which emerged about a decade ago and has found application particularly in the civil field. Safe-life design is broadly based on the concept that significant fatigue damage will not develop during the service life of the aircraft. In contrast, the fail-safe approach recognizes that some significant fatigue cracks may develop in the later stages of the life in service: design calculations are made, to be followed subsequently by tests, aimed at ensuring that the growth of any such cracks will not imperil the static strength of the structure before they are found in the course of routine inspections. The lengths of the cracks that the designer considers are based on the detection standard of inspection. The relevant inspections are generally visual (unaided) and he is dealing with cracks growing from starting lengths measured in centimetres rather than millimetres. For example, in a pressure cabin he may be asked to consider the growth of a crack from about 25 cm to a length corresponding to one frame pitch ( $\approx 50$  cm).

The approach in damage-tolerant design differs from that of fail-safe design in that the designer must assume that small crack-like flaws exist in the structure of the aircraft in the new condition, as manufactured. In essence, his problem is to predict how these cracks will grow during the service usage of the aircraft with a view to ensuring that the residual strength of the structure will not fall below an acceptable level over the required service life. It is postulated that such crack-like flaws exist at all fastener holes and at other

---

\* In this Report 'fail-safe' and 'damage-tolerant' design philosophies are given clear and distinct meanings. In general usage these distinctions are not always followed - for example, 'damage-tolerant' is sometimes used to describe both fail-safe and damage-tolerant structure as here defined.

positions in the aircraft structure, and the designer may be dealing with prediction of crack behaviour over a range of crack lengths from 0.1 mm up to as much as 50 cm. Because of the exponential nature of crack growth, much of the crack growth life will be consumed at the lower end of the crack length range, so that accuracy of prediction of crack growth behaviour at very short crack lengths is of paramount importance in the damage-tolerant design approach. This contrasts with the broad requirement stemming from fail-safe design where the crack growth prediction problem is associated with crack growth at relatively high rates towards the latter end of life. More details are given of the fail-safe and the damage-tolerant design philosophies in section 2 below.

In initiating the work described in this Report it was recognized that problems might arise in the prediction of crack growth at short crack lengths, associated with the adequacy of the analytical tools and also with the availability of appropriate data on material performance. The studies were centred on the prediction of the growth of a corner crack in an open hole in an infinite plate remotely loaded (Fig 1) with a spectrum of flight loads. Growth was predicted from a small flaw up to the point where the plate would fail due to unstable crack growth under the highest load in the spectrum. This represented, in a simplified form, one of the more searching problems of damage-tolerant design - that of demonstrating adequate life to failure from a flaw in a 'non-inspectable' part of a structure (see section 2). The effects of the variation of several parameters were studied, including initial flaw size, hole diameter and spectrum stress level. This was done for five different aluminium alloys of UK origin, having differing crack propagation and residual strength characteristics.

## 2 FAIL-SAFE AND DAMAGE-TOLERANT DESIGN - AN OUTLINE

In this section an outline is given of the 'fail-safe' and 'damage-tolerant' design philosophies. It is not intended to give a definitive statement of the different approaches and the associated airworthiness requirements but rather to give a general background to the subject, albeit at the risk of some oversimplification, so that some of the associated design problems may be understood. Readers who are familiar with the differing approaches may wish to pass directly to section 3.

In the years following World War II increasing attention was directed to the problem of fatigue in aircraft structures and the 'safe-life' philosophy of design against fatigue became generally accepted. In essence, this philosophy entails design for finite life, such that significant fatigue damage will not develop during the permitted service life of an aircraft.

In more recent years an alternative design philosophy has in some instances been used, particularly in the civil field, where the objective is to aim at achieving a 'fail-safe' structure. With this latter philosophy an aircraft is designed to have an adequate life free from significant fatigue damage but operation is permitted beyond the life at which such damage may develop. The safeguard inherent in the fail-safe approach is that any fatigue cracks that may develop will be detected by normal inspection procedures before they grow to such a length that the residual strength of the structure is reduced below a safe level. In principle, this entails first defining a crack length that cannot (reasonably) be missed in a routine service inspection. The cracks may originate from fatigue damage or from accidental damage in service and the defined lengths will generally be measured in centimetres rather than millimetres. Having defined such a crack length it is then postulated that a crack only marginally shorter has been missed at a particular inspection and that the crack will continue to grow under the appropriate service loadings until the next major inspection - perhaps one year later. It must be demonstrated to the airworthiness authorities that, over this period between inspections, the residual strength of the structure will not have fallen below a prescribed level. Safety factors are of course introduced to cover variability in loading, variability in material performance and so on. The critical parameters involved in implementing the fail-safe concept are the defined ('non-missable') crack length, the inspection period, the crack growth rate (including the crack-arrest capability of the structure) and the residual strength in the presence of a crack. The choice of materials for fail-safe structures will be biased towards those which exhibit relatively slow crack growth rates at long crack lengths; they should also have high fracture toughness so that their residual strength characteristics are good when the material is in a cracked state.

Within the last 2 to 3 years a third design philosophy has been proposed. In this the broad objective is to design a 'damage-tolerant' structure. This philosophy is in many ways similar to the fail-safe approach but it goes somewhat further in that consideration is given to crack growth from flaws which may be present in the structure as manufactured. Such flaws may arise from inherent metallurgical imperfections in the material used, or from manufacturing imperfections. The size of the flaws which must be assumed to exist are laid down in the appropriate specifications - typically, they have dimensions lying between 0.1 mm and 1.5 mm and they are assumed to be located at fastener holes and in other critical areas. In implementing the damage-tolerant approach, the component parts of the aircraft structure are assessed either to be 'inspectable' in the course of routine service inspections, or as being 'non-inspectable'. The latter

category includes parts which are not accessible for inspection without dismantling. Clearly there will be many parts of an aircraft structure that fall into this latter category - for example, the central members of a double butt-strap joint. For component parts which are assessed as 'inspectable' the procedures follow along the same general lines as for structures designed on the fail-safe philosophy, as described above. However, in the case of 'non-inspectable' parts it has to be demonstrated that the crack growth life to failure, from the prescribed initial flaw, is greater than the required service life of the aircraft. The required life may be achieved by crack-arrest (or retardation) features in the structural design or by the choice of suitable material and stress levels to give the desired slow crack growth. Bearing in mind that, under given loading conditions, crack length is an exponential function of the number of load cycles it will be evident that, in the design of 'non-inspectable' parts, attention will be focussed primarily on crack growth at short crack lengths which will occupy the greater part of life to failure.

Thus, the choice of materials for damage-tolerant structure will embrace the requirements for good crack growth and residual strength characteristics at long crack lengths, for inspectable components, as well as the requirement for favourable crack growth behaviour at very short crack lengths in the case of non-inspectable components. These differing requirements would not necessarily lead to the same material choice for both component classifications though, in practice, a compromise solution using one material is likely to be adopted.

### 3 THE PREDICTIONS

Implementation of the damage-tolerant design philosophy will involve the designer in predictions of crack growth and residual strength for a wide variety of structural components containing cracks. Such predictions will cover crack growth from specified<sup>1</sup> initial flaw (crack) sizes under stress histories appropriate to the component concerned. In seeking to gain experience of the nature of the problems likely to be encountered by the designer in carrying out such work it was decided to limit attention to one relatively simple structure/crack geometry which, it was believed, would nevertheless highlight areas of difficulty common to many more complex design situations. Attention was centred on the design problem in a 'non-inspectable' component where the objective would be to design the component so that crack growth under the applied loads, from a prescribed initial flaw, would not lead to failure of the component within twice the required service life of the aircraft. It was further postulated that the objective should be achieved by slow crack growth, rather than by crack-arrest

design features. This particular design problem embodies constraints and options in accordance with current requirements in the relevant US Military Specification<sup>1</sup>. Details of the structural model and of the applied stress history are given below.

### 3.1 The model

The structure/crack geometry chosen is illustrated in Fig 1. It consists of an infinite plate under uniaxial tensile stress,  $\sigma$ , and containing a parallel-sided hole with a single crack. The plane of the crack is normal to the surface of the plate and normal to the stress field. The initial flaw is a quarter-circle corner-crack. It is assumed to grow along the surface of the plate and down the bore of the hole until it eventually becomes a through-crack, with the crack front normal to the plate surface ('normal-to-surface through-crack'). The analytical treatment of this form of crack development, in terms of stress intensity factor, is given in Appendix A.

Under given cyclic stressing conditions, the rate at which the crack commences to grow will be a function of the size of the initial flaw - subsequently the growth rate will be strongly influenced by the diameter of the associated hole. Having this in mind, predictions of crack growth were made for three different flaw sizes and for three different hole diameters. The plate material concerned was 12.7 mm thick and calculations were made for hole diameters of 5, 10 and 15 mm. For each of these hole diameters, three different initial flaw sizes were considered: 0.125 mm ( $\approx 0.005$  in), 0.50 mm ( $\approx 0.020$  in) and 1.25 mm ( $\approx 0.050$  in). These particular flaw sizes were chosen to match prescribed flaw sizes in the US Military Specification<sup>1</sup>. For each of the foregoing combinations of hole diameter and flaw size a prediction was made of the number of stress cycles to failure under a spectrum of stress cycles derived from the load spectrum for a military aircraft operating in a training rôle (see section 3.2 below). Failure was deemed to occur when the length of the through-crack became such that the stress intensity factor at the crack tip equalled the fracture toughness value ( $K_c$ ) for the plate material concerned. The numbers of cycles to failure were subsequently expressed as fatigue lives, in terms of 'hours flown'.

### 3.2 The stress spectra

The stress spectra employed in the predictions of crack growth were based on a normal acceleration (g) spectrum which was used in the design and testing<sup>3</sup> of a military training aircraft designed on safe-life principles. For convenience the g spectrum was broken down into the following discrete acceleration ranges and associated numbers of cycles:

-1.9 g	to	5.2 g	1 cycle
-1.5 g	to	4.6 g	7 cycles
-1.0 g	to	3.9 g	27 cycles
-0.5 g	to	3.3 g	65 cycles
0 g	to	2.6 g	105 cycles
+0.4 g	to	2.0 g	195 cycles

The total number of cycles (400) represented 25 hours' flying in the training rôle.

The "stress per g" value\* for the aircraft concerned was  $4500 \text{ lb in}^{-2}$  (approximately  $31 \text{ MN m}^{-2}$ ); a service lifetime of some 5000 hours would be expected for a safe-life design with this design stress level. A stress per g of  $31 \text{ MN m}^{-2}$  was therefore used as a datum to set the stress levels in the crack growth predictions but, in order to examine the predicted effect of change in spectrum severity, additional calculations were run at values of stress per g of  $20.5 \text{ MN m}^{-2}$  ( $\approx 3000 \text{ lb in}^{-2}$ ) and  $41.5 \text{ MN m}^{-2}$  ( $\approx 6000 \text{ lb in}^{-2}$ ). As discussed below (section 3.3) calculations along the above lines were made on five different aluminium alloys to obtain some indication of their relative merits for use in damage-tolerant design. Two sets of calculations were made for each material. In the first set the spectrum severities were the same irrespective of the material and were determined from the three values of stress per g given above. However, in the second set of calculations, the values of stress per g were not the same for each material but were chosen to be fixed percentages of the ultimate tensile strength of the material concerned. The percentages chosen were based on the design situation for the military trainer aircraft mentioned above. This aircraft was made primarily from BS L65 aluminium alloy and the value of stress per g was 5.9% of the ultimate tensile stress. This provided a datum figure for the second series of calculations and set the values of 3.9%, 5.9% and 7.9% of the ultimate tensile strength to be used in assessing effects of spectrum severity.

### 3.3 Materials

The calculations of crack behaviour, as described above, were carried out for five different aluminium alloys which would be considered for use in aircraft primary structure. The materials were: BS L65, RR 58, DTD 5020, DTD 5050 and DTD 5090. The chemical compositions and tensile properties are given in Tables 1 and 2 respectively. It may be seen that BS L65 and DTD 5020 are artificially

---

\* Taken to be constant and equal to the nominal stress in the tension-surface of the wing in straight level flight.

aged, medium strength, copper-bearing alloys - DTD 5090 is a naturally aged, copper-bearing alloy, of somewhat lower strength - RR 58 is an artificially aged, medium strength, copper-magnesium alloy and DTD 5050 is an artificially aged, zinc-bearing alloy of relatively high strength. For each of the foregoing materials crack propagation data had been obtained<sup>4,5</sup> from a specimen 12.7 mm thick. The data were presented in the form of  $da/dN$  versus  $\Delta K$  curves and it was necessary to extrapolate the curves presented to cover a wider range of  $\Delta K$  (see section 4.2 below). The co-ordinates of the curves so obtained were used as direct input data for the calculations. They are listed in Table 3.

### 3.4 Method of prediction

The prediction method employed is described in some detail in Appendix B. In essence, an expression was developed for the relationship between crack length and the associated stress intensity factor ( $K$ ). Knowing this relationship, and also the applied stress spectrum, a spectrum giving the magnitude of the cyclic ranges of stress intensity factor ( $\Delta K$ ), and the associated numbers of cycles, could be obtained. Material data relating  $\Delta K$  to crack growth rate was then used to predict crack growth rate as a function of crack length, under the stress spectrum. Hence the number of stress cycles required to grow the crack from the starting flaw to critical length could be derived. The critical crack length was obtained by relating the stress intensity factor, under the maximum peak stress in the spectrum, to the fracture toughness ( $K_c$ ) for the material as deduced from extrapolation of the  $da/dN$  versus  $\Delta K$  curve. It should be noted that no allowance was made in the predictions for crack retardation effects arising from interactions of stress cycles of differing magnitudes. Several empirical models have been developed to allow for retardation effects in prediction<sup>6</sup> but it was felt that none could be used with confidence with the load spectrum concerned, containing as it does a considerable number of negative load excursions which are not considered in the retardation models.

## 4 SOME AREAS OF DIFFICULTY IN THE PREDICTIONS

In this section reference is made to difficulties which arose in making the predictions of crack growth behaviour. These difficulties were associated both with the shortcomings in analytical capability - for example in deriving values of stress intensity factor ( $K$ ) - and with inadequacies in the available materials data. In both areas there is an evident need for further work in order to improve the accuracy of design predictions for damage-tolerant structures. The difficulties which were encountered are outlined below.

#### 4.1 Analytical difficulties

The principal analytical problem was centred on the derivation of values of stress intensity factor during the transition of the crack from a quarter-circle corner-crack to a through-crack with the crack front lying normal to the plate surface. The general progress of the crack during this transition is shown in Fig 2. In the initial configuration (Fig 2a) the length of the crack as measured on the surface of the plate,  $c_1$ , is equal to the length,  $a_1$ , as measured down the bore of the hole. However, considering the stress intensity factors,  $K_b$  is greater than  $K_s$  because of the stress gradient associated with the presence of the hole. It follows therefore that the crack will tend to progress down the bore of the hole more rapidly than along the surface of the plate. In the prediction it has been assumed that the crack remains quarter-elliptical in shape with an increasing ratio of major-axis to minor-axis and that the rates of progress along the surface and down the bore are governed entirely by the instantaneous value of  $K_s$  and  $K_b$  respectively. However, it should be borne in mind that the characteristics of cyclic crack growth with stress intensity varying along the crack front have not yet been established and that, in consequence, the validity of the above assumption is open to question. Further difficulties arise in treating the transition from a quarter-elliptical crack in the bore of the hole to a normal-to-surface through-crack (Figs 2b, 2c, 2d). One of the difficulties was that, whereas stress intensity solutions were available both for the quarter-ellipse<sup>7,8</sup> and for the through-crack<sup>9</sup>, there was no solution available for the intermediate state of Fig 2c. The approach which was adopted varied with the particular circumstances. With some of the materials under the more severe stress spectra, calculations showed that the value of the stress intensity factor for the crack tip down the bore ( $K_b$ ) reached the critical  $K_c$  value for the material before this crack had reached the far surface of the plate. It was considered that when this happened catastrophic crack growth would not in fact occur, as much of the crack boundary would be well below critical conditions. It was assumed that, instead of complete failure, the crack would jump to the normal-to-surface through-crack condition. Whilst this is not regarded as an unreasonable assumption it must be made clear that there is no positive evidence to support this view - indeed there is little known about the critical conditions for a crack having varying stress intensity factor along the crack front. (This difficulty is a complementary aspect of the problem mentioned above concerning the prediction of cyclic crack growth in such circumstances.) With the less severe spectra, in many cases the crack had reached the far side of the plate before the stress intensity factor at the tip ( $K_b$ ) had reached the

critical  $K_c$  value. After considering several possible analytical approaches it was decided to assume that as the crack tip reached the far surface there would, as in the previous case, be an instantaneous jump to the normal-to-surface through-crack condition. This was probably a somewhat conservative assumption - however, when calculations were made using a notionally thicker plate, in which the crack growth down the bore was allowed to proceed beyond the true thickness of the plate until  $K_b$  equalled  $K_c$ , the results suggested that the overall reduction in life to failure from the original flaw due to this particular assumption was unlikely to exceed 10%. Again, this must be recognized as an area of uncertainty where there is an evident need for better understanding.

#### 4.2 Shortcomings in materials data

The crack-growth data were taken from experiments carried out previously at RAE and reported by Pearson<sup>4,5</sup>. They were available in the form of plots of  $da/dN$  versus  $\Delta K$  which had been determined for growth rates within the range  $2.5 \times 10^{-8}$  to  $2.5 \times 10^{-6}$  m/cycle. Pearson mentioned that 14 mm was about the maximum length of crack for which accurate calculation of  $\Delta K$  had been possible, the total distance across a specimen being approximately 25 mm. Plastic zone corrections to  $\Delta K$  had been ignored as they were very small.

The experiments had been carried out with  $R$  values of 0.05, 0.5 and 0.65. As the majority of stress cycles in the load programme considered in the present investigation had  $R$  values in the region of zero it was decided that the growth rates for  $R = 0.05$  would be adequate for use with all cycles. In order to obtain the crack-growth values required for input to the computer, each experimental growth curve was approximately represented by a series of straight lines and the co-ordinates were read at the end of each segment. Typically, about 20 segments were used to cover the whole curve including the extrapolated portions discussed below. The co-ordinates thus obtained are listed in Table 3.

The main problem involved in using the growth data was that of extrapolating the given curves beyond the limits of the experiments, since co-ordinates were required for the whole range of growth from the threshold value of  $\Delta K$  up to the point of failure. Fig 3 shows a typical example of how much extrapolation was required. Pearson had pointed out in his report that the higher values of  $\Delta K$  generally appeared to approach an asymptotic value which yielded a critical value for  $\Delta K$  corresponding well with the static fracture toughness. This fact gave some confidence in locating the failure end of a curve and each curve was therefore extrapolated to approach the appropriate asymptotic value suggested by Pearson. Slight changes in the position of this end of the curve would be

expected to affect the length of the crack at failure rather than the total number of cycles, as the crack is growing very rapidly at this stage. At the other end of the  $\Delta K$  range the situation was more uncertain, since no independent threshold values were available for the materials concerned and the establishment of a likely position for the curve was correspondingly more difficult. It was found that a variety of smooth extrapolations was possible, so a reasonable middle curve had to be adopted and the corresponding asymptote was taken as the threshold value of  $\Delta K$ . In order to obtain some idea of how much the results of the present study could be affected by this arbitrary method of selecting the threshold values, extra calculations were made for DTD 5020 material with the basic threshold value increased and decreased by 50%. It was found that with an initial crack of 0.5 mm or 1.25 mm and a value of stress per g of 31.0 or 28.0 MN m<sup>-2</sup> the changes in endurance were never more than a few per cent whichever hole diameter was being used. The changes were much greater with an initial crack of 0.125 mm, however. A 50% reduction in threshold value then produced a decrease in endurance of either 15 to 25% or 20 to 30% according to whether the stress per g was 31.0 or 28.0 MN m<sup>-2</sup> respectively. For a 50% increase in threshold value the corresponding increases in endurance were 50 to 75% and 100 to 150% respectively. In all cases the changes were greatest for the largest hole. It must be noted that these values would not necessarily be applicable to other materials.

## 5 PRESENTATION AND DISCUSSION OF RESULTS

### 5.1 General

A complete set of results is presented in Table 4. The table shows predicted endurance to failure, expressed in flying hours, for the five materials considered under the various combinations of spectrum severity, hole diameter, and initial crack length. The spectrum severity is given in terms of the stress per g.

In the upper half of the table the results are given for the five materials using the same three values of stress per g for each material - the results in the lower half give the endurances when the value of stress per g is scaled to 5.9% of the ultimate tensile strength of each different material (section 3.2 above refers).

The overall pattern of results for a value of stress per g of 31 MN m<sup>-2</sup> is illustrated graphically in Fig 4, which also includes values of critical crack length under the maximum load in the spectrum. (The critical crack lengths would be shorter if failure were related to a somewhat more severe loading condition, eg proof load, but the lives to failure would not be significantly curtailed, due

to the exponential nature of crack growth.) In looking at the results presented, too much weight should not be placed on the apparent differences in performance achieved by each of the five materials. Broadly, there are two reasons for saying this. Firstly, the available crack propagation data for each material were based on tests on one batch of plate only and it was not possible to assess how typically the available data reflected the general performance of the material concerned. Secondly, as discussed in section 4.2 above, it was necessary in performing the calculations for each material to extrapolate well outside the experimentally established data points. The assessment of the relative performance of the materials should therefore be regarded as qualitative rather than quantitative.

Nevertheless, certain broad observations may be made from a study of Fig 4. Firstly, as would be expected, endurance is reduced by increase in initial crack length - the magnitude of the reduction is influenced by hole diameter. Secondly, for a given initial crack length, life is reduced by increase in hole diameter, the amount of the reduction being apparently related to the initial crack length. Thirdly, there does not appear to be a clear-cut correlation between the fracture toughness of the material ( $K_c$ ), as reflected in the crack length at failure, and the relative endurance of the different materials. A final observation may be made that the lives achieved at this spectrum severity (value of stress per g:  $31 \text{ MN m}^{-2}$ ,  $4500 \text{ lb in}^{-2}$ ) would not, in general, be regarded by a designer as adequate bearing in mind that, by specification, he is looking for a factor of two on service life (see also section 5.2 below).

Fig 5 gives corresponding results when the values of stress per g have been adjusted to give levels of 5.9% of the ultimate tensile strength of each material concerned. In the case of RR 58, DTD 5020 and DTD 5090, there has been a consequent reduction in spectrum severity with an associated marked increase in life. This is of course at the expense of some weight increase - the percentage weight changes may be obtained by simply assuming that the weight of the structure is inversely proportional to the operating values of stress per g noted on the figure. It will be seen from this figure that, notwithstanding the evident changes in endurance, the observations made from a study of Fig 4 need not be significantly modified.

Further amplification of the observations made above is included in the sections which follow.

## 5.2 Effect of spectrum severity on endurance

From the predicted values of endurance given in Table 4 it is evident that the effect of change in the value of stress per g (ie change in spectrum severity) is conditioned both by the associated hole diameter and by the initial crack length. In order to give an indication of the general relationship between endurance and spectrum severity, the results for a 10mm hole with two different initial crack lengths, 0.125 mm and 1.25 mm, are examined in this section.

The format of presentation is very similar to that of the presentation of conventional S/N curves. Points are plotted, based on data in Table 4, showing endurance to failure at a number of values of stress per g, the endurance being given in terms of the predicted number of flying hours for the crack to grow from the specified initial length to the length at which fast fracture would occur under the highest load in the spectrum. Fig 6 shows the data points giving the relationship between endurance and spectrum severity, for the five different materials, when the initial crack length is 0.125 mm. Upper and lower bounds are given which embrace these data points. It will be seen that in the central part of the endurance range ( $10^4$  cycles) the different performances of the five materials fall within a range of values of stress per g which is approximately  $\pm 10\%$  of the mean 1g stress level at that endurance. Also included in the figure is a line (dashed) showing the shape of the relationship between stress and endurance if the endurance is taken to be inversely proportional to the sixth power of stress. It will be seen that this line closely approximates to the shape of the upper and lower boundary curves. Finally, it may be noted that, taking an average (log mean) of the performance of all five materials, a life to failure of 10000 hours is predicted at a value of stress per g of  $31 \text{ MN m}^{-2}$  ( $4500 \text{ lb in}^{-2}$ ) for this combination of hole diameter and initial crack length.

Corresponding results for the 10mm diameter hole, but with a 1.25mm initial crack, are shown in Fig 7. As in the preceding figure, upper and lower bounds are shown (solid lines) which embrace the majority of the data points. It will be seen that at the highest 1g stress level no data points are plotted for the RR 58, DTD 5020 and DTD 5050 materials: this was because they would reach the critical  $K_c$  value, for an initial crack length of 1.25 mm, at a stress level somewhat lower than the peak stress in the spectrum during the first application of the spectrum of loads. The upper bound indicates a relationship of endurance to stress approximating to an inverse fifth power law - the lower bound indicates an inverse eighth power law. As would be anticipated, the predicted lives to failure at a given spectrum level are much lower for an initial crack length of

1.25 mm than for a 0.125mm crack. Again taking the average performance of the five materials, a life of approximately 2500 hours is predicted at a value of stress per g of  $31 \text{ MN m}^{-2}$ , compared with 10000 hours for the shorter initial crack.

The aim in damage-tolerant design<sup>1</sup> is to achieve twice the service lifetime before the strength of the structure is reduced below an acceptable level. It will be seen from the above predictions that, in the case of an initial crack length of 1.25 mm at a 10mm hole, the life of a component is likely to be unsatisfactory. In such circumstances it would be necessary to reduce the lg stress level, with a consequent weight increase for the component concerned. For example, with the above hole/crack geometry, it would apparently be necessary to keep the value of stress per g below  $24 \text{ MN m}^{-2}$  ( $3500 \text{ lb in}^{-2}$ ) in order to achieve a service life of 5000 hours. This contrasts with a value of stress per g of  $31 \text{ MN m}^{-2}$  ( $4500 \text{ lb in}^{-2}$ ) used in the (safe-life) design of the trainer aircraft from which the datum stress levels used in this study were obtained. This assessment may, however, be unduly pessimistic as no allowance has been made for any retardation effects on crack growth (see section 3.4 above) and it would be unwise to place too much emphasis on the conclusions drawn, pending evidence on the magnitude of such effects in the materials and plate thickness concerned.

### 5.3 Influence of hole diameter and initial crack length on endurance

In the foregoing discussion mention has been made of the effects of both hole diameter and initial crack length on predicted endurance to failure; it was also noted that the magnitudes of such effects were dependent on these two parameters jointly. In Fig 8 the results of the predictions for all five materials have been grouped together to indicate the effect on endurance of varying hole diameter and initial crack length, respectively. The hatched areas on the figures cover the results for the different materials. A value of stress per g of  $31 \text{ MN m}^{-2}$  was used in the associated predictions of endurance.

It is evident from Fig 8a that increase in hole diameter reduces endurance and that the effect is more significant for the longer initial crack lengths. Correspondingly, in Fig 8b, it is seen that the effect of increase in initial crack length is more marked for the larger hole diameters.

## 6 CONCLUDING OBSERVATIONS

Implementation of the damage-tolerant design philosophy will entail the prediction of crack growth from small crack-like flaws in the structure. The study presented in this Report was undertaken in order to obtain some experience of the nature of the problems involved in such work and also to obtain some feel

for the effect on endurance of variation of some of the parameters concerned. Attention was centred on the behaviour of a corner-crack growing from a hole in plate material. Predictions were made for five different aluminium alloys under a spectrum of flight loads. The main points which arose during the study and the conclusions reached are summarised below:

- (1) No firmly established analytical method is available to describe the growth of a corner-crack at a hole into a through-crack in the surrounding plate material.
- (2) The evolution of a suitable analytical method, in the course of the work described, involved assumptions concerning crack propagation and residual strength when the stress intensity factor is not constant along the crack front. The physical behaviour of a crack in such circumstances is not yet understood.
- (3) Calculations of crack growth necessitated the use of  $da/dN$  versus  $\Delta K$  data covering a range of  $\Delta K$  from the threshold value  $\Delta K_{\text{threshold}}$  up to  $K_{\text{max}}$  equal to  $K_c$ . The available data on the five materials concerned did not cover rates below  $2.5 \times 10^{-8}$  m/cycle and extrapolation to approximately  $10^{-9}$  m/cycle was necessary. Errors in extrapolation could have a significant effect on predicted endurance; eg 50% error in the value assumed for  $\Delta K_{\text{threshold}}$  could result in a 2:1 error in predicted endurance.
- (4) The crack propagation data available for the five materials had been measured on one batch only of each material. It was therefore not possible to be sure how typical the data were for the materials concerned.
- (5) It was felt that none of the existing crack retardation models could be used with confidence in the predictions, therefore no allowance for any such effects was made.
- (6) The study, which included variation of material, spectrum severity, hole diameter and initial crack length, showed a strong effect on predicted endurance of variation in any one of these parameters. Additionally, it showed a marked interaction between the parameters in their combined effect on endurance. Some examples follow:
  - (i) Change of material: the band of results for the five materials embraced a 6:1 change in endurance for a 1.25mm initial crack, at a 10mm diameter hole, with a value of stress per g of  $31 \text{ MN m}^{-2}$ . The effect was less for a 0.125mm initial crack.

(ii) Value of stress per g: predicted endurance was inversely proportional to  $(\text{stress per g})^n$ , where  $n$  ranged from 5 to 8 depending on the material concerned, for a 1.25mm crack from a 10mm diameter hole.

(iii) Hole diameter: for an initial crack length of 1.25 mm and a lg spectrum level of  $31 \text{ MN m}^{-2}$ , increase of hole diameter from 5 mm to 15 mm reduced life by a factor of five (average result for all materials). The effect was less for a 0.125mm initial crack length.

(iv) Initial crack length: with a 10mm hole and a value of stress per g of  $31 \text{ MN m}^{-2}$  a change of initial length from 0.125 mm to 1.25 mm reduced life by a factor of four (average result for all materials). The effect was less with a smaller hole and greater with a larger hole.

(7) When implementing the damage-tolerant design philosophy it may be necessary to reduce the values of stress per g to levels below those used in safe-life design. This may entail a significant weight penalty.

It is evident from the above observations that experimental research studies are desirable in order to resolve the uncertainties which became apparent in carrying out the analytical work. Experimental work is also required to check the overall soundness of the conclusions reached.

Appendix A

DERIVATION OF STRESS INTENSITY FACTORS

The stress intensity factors were derived after reference to Paris and Sih<sup>10</sup>, who dealt with semi-elliptical surface flaws in a plate, and to Broek *et al*<sup>7</sup> and Shah<sup>8</sup> who further considered quarter-elliptical corner flaws at a hole in a plate. In general they all started from the factor for an ellipse embedded in an infinite solid and then incorporated suitable adjustments to allow for the presence of a hole and the effects of the front and back surfaces of a plate.

Broek and Paris and Sih quoted Irwin's factor<sup>11</sup> for an embedded ellipse which, in the notation of Fig 9, gives

$$K = \frac{\sigma}{\phi} \sqrt{\pi a} \left( \frac{a^2}{c^2} \cos^2 \psi + \sin^2 \psi \right)^{\frac{1}{4}}$$

where  $\phi$  is the elliptical integral given by

$$\phi = \int_0^{\pi/2} \left[ 1 - \left( \frac{c^2 - a^2}{c^2} \right) \sin^2 \theta \right]^{\frac{1}{2}} d\theta .$$

Irwin also suggested a correction for plastic-zone size, but this has not been incorporated into the present calculations. It is seen that at the end of the semi-major axis of length  $c$ ,  $\psi = 0$  and

$$K = \frac{\sigma}{\phi} \sqrt{\pi a} \sqrt{\frac{a}{c}} = \frac{\sigma}{\phi} \frac{a}{c} \sqrt{\pi c}$$

and at the end of the semi-minor axis of length  $a$ ,  $\psi = \pi/2$  and

$$K = \frac{\sigma}{\phi} \sqrt{\pi a} .$$

The separation of two halves of the ellipse by a circular hole introduces an increase in stress intensity arising from the stress concentration around the hole and from the free edge at the hole boundary. Bowie's factors<sup>9</sup> covering these effects for a through-crack from a hole have been taken to be adequate for an elliptical crack also and have therefore been included in the calculation.

The reduction of an embedded ellipse to a semi-ellipse at a free surface introduces a free-surface effect. The usually accepted factor<sup>10</sup> of 1.12 for

through-cracks needs to be modified to allow for the geometry of an elliptical flaw. Paris and Sih suggested  $1 + 0.12(1 - a/c)$  for the deepest point of the flaw and Shah suggested  $1 + 0.12(1 - a/2c)^2$  with negligible variation around the periphery of the flaw. In both cases  $c$  was the semi-axis lying along the surface.

For the effect of the back surface of the plate both Broek and Shah recommended the factors derived by Kobayashi<sup>12</sup> and presented graphically by Wilhem<sup>13</sup>.

In the investigation reported here the initial flaw was required to be quarter-circular. From Irwin's formula given above, the stress intensity of an embedded circle of radius  $r$  is equal for all points on the circumference and has a value  $K = (\sigma/\phi)\sqrt{\pi r}$ . The suggested front-surface corrections will lie between 1.0 and 1.03 for this case, so may be taken as 1.0 approximately, and the back-surface correction also proves to be 1.0. The only difference between the stress intensities at the points where a quarter-circular flaw meets the boundary of the hole and the surface of the plate will therefore be that arising from the difference in Bowie's factor for those points. Since that factor has its greatest value of 3.39 at the boundary of the hole and the stress intensity will consequently be greatest there, it follows that the flaw will grow faster along the bore of the hole than along the surface of the plate and that the resulting quarter-ellipse will have its semi-minor axis along the surface. For this orientation of the ellipse the front and back surface correction factors remain at a value of 1.0.

To maintain comparability with the more usual case of shallow surface-flaws, the crack length along the surface was still called  $c$  even though it had become the semi-minor axis of an ellipse. Taking this fact into account, the final expressions used in the calculations therefore became:

$$K_{\text{surface}} = \frac{\sigma}{\phi} \sqrt{\pi c} \times (\text{Bowie factor for single crack of length } c)$$

$$K_{\text{bore}} = \frac{\sigma c}{\phi a} \sqrt{\pi a} \times 3.39$$

where  $\phi$  was now given by

$$\phi = \int_0^{\pi/2} \left[ 1 - \left( \frac{a^2 - c^2}{a^2} \right) \sin^2 \theta \right]^{\frac{1}{2}} d\theta .$$

## Appendix B

### DESCRIPTION OF PREDICTION METHOD

In general, since the growth of a fatigue crack is related to the applied alternating stress intensity  $\Delta K$ , approximate calculations of crack life can be made by considering arbitrarily-selected increments in crack length and calculating for each increment a suitable average value of  $\Delta K$ , the corresponding average rate of growth per loading cycle and thence the approximate number of cycles required for the crack to grow through the increment.

The particular flaw considered in this Report is required to be quarter-circular initially, but consideration of the stress-intensity factors (see Appendix A) suggests that the flaw will grow into a quarter-ellipse having its semi-minor axis, of length  $c$ , along the surface of the plate and its semi-major axis, of length  $a$ , along the bore of the hole through the plate. Growth therefore has to be considered along both semi-axes simultaneously, and the two surfaces of the crack will be referred to here as 'surface-crack' and 'bore-crack' for convenience.

Appendix A shows that the stress intensities and hence the crack growth rates for a corner flaw involve parameters which are dependent on the elliptical-shape ratio  $c/a$ , so in order to make crack life calculations of the kind outlined above it is necessary to know the value of that ratio beforehand. Since the shape of the ellipse gradually changes as the crack grows, however, the shape-ratio cannot be accurately predicted and it becomes necessary to choose the increment arbitrarily for one surface only and to make a reasonable estimate of the corresponding increment along the other surface. Provisional values of stress intensity can then be calculated and used to obtain probable rates of growth in both directions, after which calculations can be made first of the number of cycles required for growth through the chosen increment and then of the amount of simultaneous growth along the other surface. If the latter, calculated increment is in reasonable agreement with its previously estimated value it is assumed that the various parameters used in the calculation of  $\Delta K$  were sufficiently accurate for the calculated increment and number of cycles to be valid. Otherwise a refined estimate of that increment is made, lying between the previous estimate and the resultant calculated value, and the whole calculation is repeated as necessary until the estimated and calculated values have converged to a desired extent. The process is then applied to succeeding increments in their turn.

When the bore-crack either reaches the far side of the plate or produces a maximum stress intensity which is greater than the critical value for the material, it is assumed that the quarter-elliptical crack immediately jumps to become a through-crack having the same length as the existing surface-crack. Calculations are then continued for growth along the surface, using stress intensity factors appropriate to the through-crack, until the critical stress intensity is reached in that direction, at which stage final failure is assumed to occur.

The computer programme written for the study described in this Report assumes that the fatigue loading is given in the form of a specified spectrum of load cycles but that the cycles are not applied in any particular order. Rather, calculations are based on 'weighted average' growth per cycle as defined in (8) below. Linear summation of damage is therefore assumed to occur and no account is taken of any change arising from load-sequence effects. It is further assumed that crack-growth takes place only during the positive portion of a load cycle and that it follows either Pearson's modification<sup>4,5</sup> of Forman's growth law or any experimental crack-growth curve given in terms of fracture mechanics.

Details incorporated into the computer program include the following:

- (1) Increments along the surface of the plate are selected arbitrarily and the corresponding increments down the bore of the hole are calculated.
- (2) The ratio between successive surface-increments is kept constant at a pre-selected value unless the crack is about to extend through the plate or the critical stress intensity is being closely approached along either crack-surface. At those stages smaller increments are selected so as to approximate fairly closely to the required or critical length.
- (3) All variable parameters used in the crack-growth calculation for a given increment are related to the mean crack lengths during the increment.
- (4) In order that the necessary estimates of bore-increment may be made it is assumed at first that the elliptical-shape ratio is reduced from 1.0 to an average of 0.99 for the first increment and is then reduced for subsequent increments in geometric progression from previously established values. The assumed ratio is subsequently modified each time the bore-increment is re-estimated.
- (5) When the bore-crack has exceeded or seems likely to exceed the thickness of the material, the estimated bore-increment is reduced to the value which would make the bore-crack just equal to the thickness and the selected surface-increment is reduced proportionately. Because of the iterative nature of the calculation it will probably not be possible to make the final length of

bore-crack equal the thickness of the material exactly without unduly prolonging the calculations, so the programme allows the crack to become a few per cent greater than the thickness if necessary. Where this occurs, it can help to balance the lack of allowance for any transition period between the breaking-through of the corner flaw and the full establishment of the through-crack.

(6) The values of Bowie's factor and  $\phi$  required in the calculation of stress intensities are computed by linear interpolation between input data values.

(7) Before the crack-growth is calculated for any increment, a calculation is made of the maximum stress intensities resulting from the application of the highest stress level to the expected crack lengths at the end of the increment, to determine whether they exceed the critical stress intensity for the material. If the critical level is being attained in the bore-crack, up to three attempts are made to reduce the maximum intensity below critical level by slightly adjusting the estimated bore-increment. If these attempts are unsuccessful, or if the critical level is being attained by a surface-crack or a through-crack, the chosen surface-increment is progressively halved, all other dependent parameters being adjusted each time, until a non-critical maximum stress intensity is achieved and the crack-growth calculation can proceed. When ten such halvings have been made altogether it is assumed that critical stress intensity can no longer be avoided and that the crack will then proceed to the stage of either through-crack or final failure, depending on whether the critical intensity is arising in the hole or at the surface of the plate respectively.

(8) For the calculation of the weighted average crack-growth per cycle the value of  $\Delta K$  appropriate to the surface being considered is first calculated for each stress level in turn, ignoring negative parts of the stress cycle. The corresponding rates of crack-growth are then calculated, either from the Pearson-Forman equation<sup>4,5</sup> or by linear interpolation between input co-ordinates from an experimental growth curve. Finally, the growth rates are combined in proportion to the numbers of cycles of the associated stress levels within the whole spectrum.

(9) The validity of the crack-growth calculation is accepted when the calculated bore-increment comes within 10% of its estimated value.

(10) If it is found at any stage that the number of cycles required to complete the last increment was less than ten or that the current increment requires less than one cycle, it is assumed that the crack is progressing so rapidly that final failure is imminent and no further calculation is made.

Table 1

CHEMICAL COMPOSITIONS (NOMINAL)

Material	Heat treatment	Nominal composition %							
		Cu	Mg	Mn	Zn	Si	Cr	Ni	Fe
BS L65	Artificially aged	4.4	0.6	0.8	-	0.7	-	-	-
RR 58	Artificially aged	2.5	1.5	-	-	0.2	-	1.2	1.0
DTD 5020	Artificially aged	4.4	0.7	0.6	-	0.7	-	-	-
DTD 5050	Artificially aged	0.9	2.7	-	5.7	-	0.2	-	-
DTD 5090	Naturally aged	4.4	1.5	0.6	-	-	-	-	-

Table 2

TENSILE PROPERTIES (MEASURED)

	BS L65	RR 58	DTD 5020	DTD 5050	DTD 5090
0.1% PS, MN m <sup>-2</sup>	482	404	435	515	374
0.2% PS, MN m <sup>-2</sup>	490	414	442	525	376
Tensile strength, MN m <sup>-2</sup>	524	445	476	573	484
Elongation on $4\sqrt{a}$ %	10.5	10.5	14	15.4	18
Static fracture toughness, MN m <sup>-3/2</sup>		23	28	28	44
K <sub>c</sub> derived from crack growth rate curves, MN m <sup>-3/2</sup>	31.6	26.4	26.4	27.5	40.7

Table 3

## CO-ORDINATES OF CRACK-GROWTH CURVES

L65		RR 58		DTD 5020		DTD 5050		DTD 5090	
$\Delta K$	$\log \frac{da}{dN}$								
<i>1.90</i>	<i>-11.30</i>	<i>5.00</i>	<i>-8.86</i>	<i>3.35</i>	<i>-9.50</i>	<i>4.50</i>	<i>-8.90</i>	<i>4.00</i>	<i>-9.50</i>
<i>2.00</i>	<i>-10.94</i>	<i>5.15</i>	<i>-8.71</i>	<i>3.40</i>	<i>-9.14</i>	<i>4.55</i>	<i>-8.68</i>	<i>4.10</i>	<i>-9.18</i>
<i>2.20</i>	<i>-10.34</i>	<i>5.20</i>	<i>-8.44</i>	<i>3.55</i>	<i>-8.99</i>	<i>4.70</i>	<i>-8.42</i>	<i>4.20</i>	<i>-8.95</i>
<i>2.50</i>	<i>-9.80</i>	<i>5.50</i>	<i>-8.16</i>	<i>3.75</i>	<i>-8.75</i>	<i>5.15</i>	<i>-8.01</i>	<i>4.65</i>	<i>-8.53</i>
<i>2.90</i>	<i>-9.32</i>	<i>5.80</i>	<i>-7.97</i>	<i>4.10</i>	<i>-8.44</i>	<i>5.90</i>	<i>-7.62</i>	<i>5.10</i>	<i>-8.29</i>
<i>3.50</i>	<i>-8.84</i>	<i>6.15</i>	<i>-7.78</i>	<i>4.50</i>	<i>-8.20</i>	<i>7.05</i>	<i>-7.22</i>	<i>5.55</i>	<i>-8.06</i>
<i>4.00</i>	<i>-8.49</i>	<i>6.70</i>	<i>-7.56</i>	<i>5.00</i>	<i>-7.99</i>	<i>7.70</i>	<i>-7.05</i>	<i>6.30</i>	<i>-7.78</i>
<i>4.55</i>	<i>-8.22</i>	<i>7.20</i>	<i>-7.43</i>	<i>5.65</i>	<i>-7.74</i>	<i>8.60</i>	<i>-6.89</i>	<i>7.10</i>	<i>-7.55</i>
<i>5.20</i>	<i>-7.96</i>	<i>7.90</i>	<i>-7.29</i>	<i>6.55</i>	<i>-7.52</i>	<i>9.55</i>	<i>-6.75</i>	<i>8.45</i>	<i>-7.20</i>
<i>5.85</i>	<i>-7.72</i>	<i>8.50</i>	<i>-7.19</i>	<i>8.00</i>	<i>-7.24</i>	<i>10.80</i>	<i>-6.61</i>	<i>10.20</i>	<i>-6.84</i>
<i>6.60</i>	<i>-7.49</i>	<i>9.70</i>	<i>-7.04</i>	<i>9.65</i>	<i>-6.97</i>	<i>12.85</i>	<i>-6.42</i>	<i>11.70</i>	<i>-6.60</i>
<i>7.50</i>	<i>-7.28</i>	<i>10.90</i>	<i>-6.92</i>	<i>10.95</i>	<i>-6.79</i>	<i>19.60</i>	<i>-5.91</i>	<i>13.30</i>	<i>-6.39</i>
<i>8.50</i>	<i>-7.07</i>	<i>13.50</i>	<i>-6.70</i>	<i>12.60</i>	<i>-6.61</i>	<i>20.80</i>	<i>-5.80</i>	<i>14.60</i>	<i>-6.26</i>
<i>9.70</i>	<i>-6.85</i>	<i>17.05</i>	<i>-6.35</i>	<i>13.60</i>	<i>-6.51</i>	<i>21.70</i>	<i>-5.68</i>	<i>16.30</i>	<i>-6.12</i>
<i>11.20</i>	<i>-6.60</i>	<i>18.00</i>	<i>-6.24</i>	<i>14.90</i>	<i>-6.41</i>	<i>22.90</i>	<i>-5.49</i>	<i>18.65</i>	<i>-5.95</i>
<i>12.60</i>	<i>-6.40</i>	<i>19.50</i>	<i>-6.04</i>	<i>17.40</i>	<i>-6.26</i>	<i>24.10</i>	<i>-5.24</i>	<i>20.00</i>	<i>-5.87</i>
<i>14.20</i>	<i>-6.19</i>	<i>20.50</i>	<i>-5.89</i>	<i>18.60</i>	<i>-6.18</i>	<i>24.65</i>	<i>-5.07</i>	<i>23.50</i>	<i>-5.72</i>
<i>15.50</i>	<i>-6.02</i>	<i>21.40</i>	<i>-5.73</i>	<i>19.95</i>	<i>-6.07</i>	<i>25.15</i>	<i>-4.83</i>	<i>26.15</i>	<i>-5.58</i>
<i>20.80</i>	<i>-5.40</i>	<i>22.60</i>	<i>-5.51</i>	<i>20.80</i>	<i>-5.99</i>	<i>25.60</i>	<i>-4.54</i>	<i>28.15</i>	<i>-5.45</i>
<i>22.40</i>	<i>-5.19</i>	<i>23.20</i>	<i>-5.39</i>	<i>21.55</i>	<i>-5.88</i>	<i>25.85</i>	<i>-4.30</i>	<i>30.15</i>	<i>-5.30</i>
<i>23.85</i>	<i>-4.96</i>	<i>23.90</i>	<i>-5.17</i>	<i>22.45</i>	<i>-5.71</i>	<i>26.00</i>	<i>-4.06</i>	<i>31.70</i>	<i>-5.15</i>
<i>25.00</i>	<i>-4.74</i>	<i>24.40</i>	<i>-4.93</i>	<i>23.05</i>	<i>-5.57</i>	<i>26.05</i>	<i>-3.83</i>	<i>33.05</i>	<i>-5.01</i>
<i>25.80</i>	<i>-4.55</i>	<i>24.75</i>	<i>-4.70</i>	<i>23.60</i>	<i>-5.42</i>	<i>26.10</i>	<i>-3.70</i>	<i>34.30</i>	<i>-4.85</i>
<i>26.55</i>	<i>-4.34</i>	<i>24.95</i>	<i>-4.40</i>	<i>24.05</i>	<i>-5.21</i>			<i>35.05</i>	<i>-4.74</i>
<i>27.25</i>	<i>-4.07</i>	<i>25.05</i>	<i>-4.21</i>	<i>24.50</i>	<i>-4.98</i>			<i>35.70</i>	<i>-4.63</i>
<i>27.50</i>	<i>-3.85</i>	<i>25.10</i>	<i>-3.86</i>	<i>24.75</i>	<i>-4.75</i>			<i>36.50</i>	<i>-4.45</i>
<i>28.40</i>	<i>-3.49</i>			<i>24.95</i>	<i>-4.53</i>			<i>37.25</i>	<i>-4.22</i>
<i>28.80</i>	<i>-3.14</i>			<i>25.05</i>	<i>-4.27</i>			<i>37.75</i>	<i>-3.98</i>
<i>29.30</i>	<i>-2.67</i>			<i>25.10</i>	<i>-4.00</i>			<i>38.30</i>	<i>-3.63</i>
<i>29.65</i>	<i>-2.19</i>							<i>38.55</i>	<i>-3.35</i>
<i>29.85</i>	<i>-1.72</i>							<i>38.70</i>	<i>-2.90</i>
<i>31.60</i>	<i>+1.00</i>								

Notes: The figures given in italics were obtained by extrapolation from the measured values.

$\Delta K$  was measured in  $\text{MN}/\text{m}^{\frac{3}{2}}$  and  $da/dN$  in  $\text{m}/\text{cycle}$  (as indicated in Fig 3).

Table 4  
PREDICTED HOURS TO FAILURE

Material		BS L65			RR 58			DTD 5020			DTD 5050			DTD 5090		
Hole diameter	Initial crack length	Stress per g - MN/m <sup>2</sup> (lbf/in <sup>2</sup> )			Stress per g - MN/m <sup>2</sup> (lbf/in <sup>2</sup> )			Stress per g - MN/m <sup>2</sup> (lbf/in <sup>2</sup> )			Stress per g - MN/m <sup>2</sup> (lbf/in <sup>2</sup> )			Stress per g - MN/m <sup>2</sup> (lbf/in <sup>2</sup> )		
		20.5 (3000)	31.0 (4500)	41.5 (6000)												
5mm	0.125mm	54200	7520	1710	∞	16900	2730	78400	9690	2000	∞	8430	1490	312000	14300	3700
	0.50mm	27800	4210	763	50800	7670	1200	35600	6200	917	26000	4360	706	44600	7680	2270
	1.25mm	20700	2940	343	37400	5690	242	28400	4670	240	19400	3400	220	32000	5920	1810
	(Approximate failure length)	(50mm)	(20mm)	(7mm)	(35mm)	(13mm)	(2.5mm)	(35mm)	(13mm)	(2.5mm)	(38mm)	(14mm)	(3mm)	(85mm)	(36mm)	(19mm)
10mm	0.125mm	35000	4260	1080	∞	9340	1790	53600	4780	1290	>227000	4550	924	175000	9450	2030
	0.50mm	14500	1600	313	27200	2620	534	20300	1990	399	14500	1480	295	25000	4320	866
	1.25mm	10300	836	54	20200	1290	-	15800	955	-	11100	823	-	18100	3330	562
	(Approximate failure length)	(49mm)	(10mm)	(2mm)	(32mm)	(4mm)	(1mm)	(32mm)	(4mm)	(1mm)	(35mm)	(5mm)	(1mm)	(83mm)	(33mm)	(9mm)
15mm	0.125mm	28600	3600	946	∞	7980	1570	41700	3950	1150	>190000	3760	825	167000	7420	1580
	0.50mm	9440	1090	215	16400	1810	407	12500	1320	313	9150	972	227	18500	2640	544
	1.25mm	6140	478	-	10900	725	-	8890	504	-	6460	419	-	13100	1870	296
	(Approximate failure length)	(43mm)	(4mm)	(1.5mm)	(21mm)	(2mm)	(1mm)	(21mm)	(2mm)	(1mm)	(25mm)	(2mm)	(1mm)	(82mm)	(23mm)	(4mm)

Hole diameter	Initial crack length	Stress per g - MN/m <sup>2</sup> (lbf/in <sup>2</sup> )			Stress per g - MN/m <sup>2</sup> (lbf/in <sup>2</sup> )			Stress per g - MN/m <sup>2</sup> (lbf/in <sup>2</sup> )			Stress per g - MN/m <sup>2</sup> (lbf/in <sup>2</sup> )			
		31.0 (4500)			26.5 (3800)			28.0 (4000)			34.0 (4900)			28.5 (4100)
5mm	0.125mm		7520			69600					4850			22200
	0.50mm		4210			16400					2710			10700
	1.25mm		2940			13000					1960			8270
	(Approximate failure length)		(20mm)			(20mm)					(10mm)			(43mm)
10mm	0.125mm		4260			37900					2540			15000
	0.50mm		1600			6510					850			6220
	1.25mm		836			4300					361			4790
	(Approximate failure length)		(10mm)			(11mm)					(3mm)			(41mm)
15mm	0.125mm		3600			31500					2170			12100
	0.50mm		1090			3870					610			4150
	1.25mm		478			2040					203			3000
	(Approximate failure length)		(4mm)			(4mm)					(2mm)			(34mm)

REFERENCES

- | <u>No.</u> | <u>Author</u>                          | <u>Title, etc</u>  |
|------------|--|--|
| 1          | -                                      | Airplane damage tolerance requirements.<br>Military Specification MIL-A-83444 (USAF) (1974)  |
| 2          | R.D.J. Maxwell                         | The practical implementation of fatigue requirements to military aircraft and helicopters in the United Kingdom. Proceedings of 6th ICAF Symposium, Miami, May 1971<br>NASA SP-309 pp 213-229 (1972)             |
| 3          | H.E. Parish                            | Fatigue test results and analysis of 42 Piston Provost wings.<br>Unpublished MOD material (1965)   |
| 4          | S. Pearson                             | The effect of mean stress on fatigue crack propagation in half-inch thick specimens of aluminium alloys of high and low fracture toughness.<br>Eng. Fract. Mech., Vol 4, pp 9-24 (1972)                          |
| 5          | S. Pearson                             | Initiation of fatigue cracks in commercial aluminium alloys and the subsequent propagation of very short cracks.<br>RAE Technical Report 72236 (ARC 34684) (1973)  |
| 6          | H. Liebowitz<br>(Editor)               | Fracture mechanics of aircraft structures.<br>AGARDograph No.176, pp 173-179   |
| 7          | D. Broek<br>A. Nederveen<br>A. Meulman | Applicability of fracture toughness data to surface flaws and to corner cracks at holes.<br>NLR TR 71033U (1971)   |
| 8          | R.C. Shah                              | Stress intensity factors for through and part-through cracks originating at fastener holes.<br>Paper presented at Eighth National Symposium on Fracture Mechanics, Brown University, Providence, RI, August 1974 |
| 9          | O.L. Bowie                             | Analysis of an infinite plate containing radial cracks originating from the boundary of an internal circular hole.<br>J. of Mathematics and Physics, <u>35</u> , pp 60-71 (1956)                                 |
| 10         | P.C. Paris<br>G.C. Sih                 | Stress analysis of cracks.<br>ASTM STP 381, pp 30-81 (1965)  |

REFERENCES (concluded)

<u>No.</u>	<u>Author</u>	<u>Title, etc</u>
11	G.R. Irwin	Crack extension force for a part-through crack in a plate. J. Appl. Mech., Vol 29, pp 651-654 (1962)
12	A.S. Kobayashi M. Zir L. Hall	Approximate stress intensity factor for an embedded elliptical crack near two parallel free surfaces. Int. J. Fracture Mechanics, Vol 1, No.9, pp 81-95 (1965)
13	D.P. Wilhem	Fracture mechanics guidelines for aircraft structures applications. AFFDL-TR-69-111 (1970)

*Reports quoted are not necessarily available to members of the public or to commercial organisations*

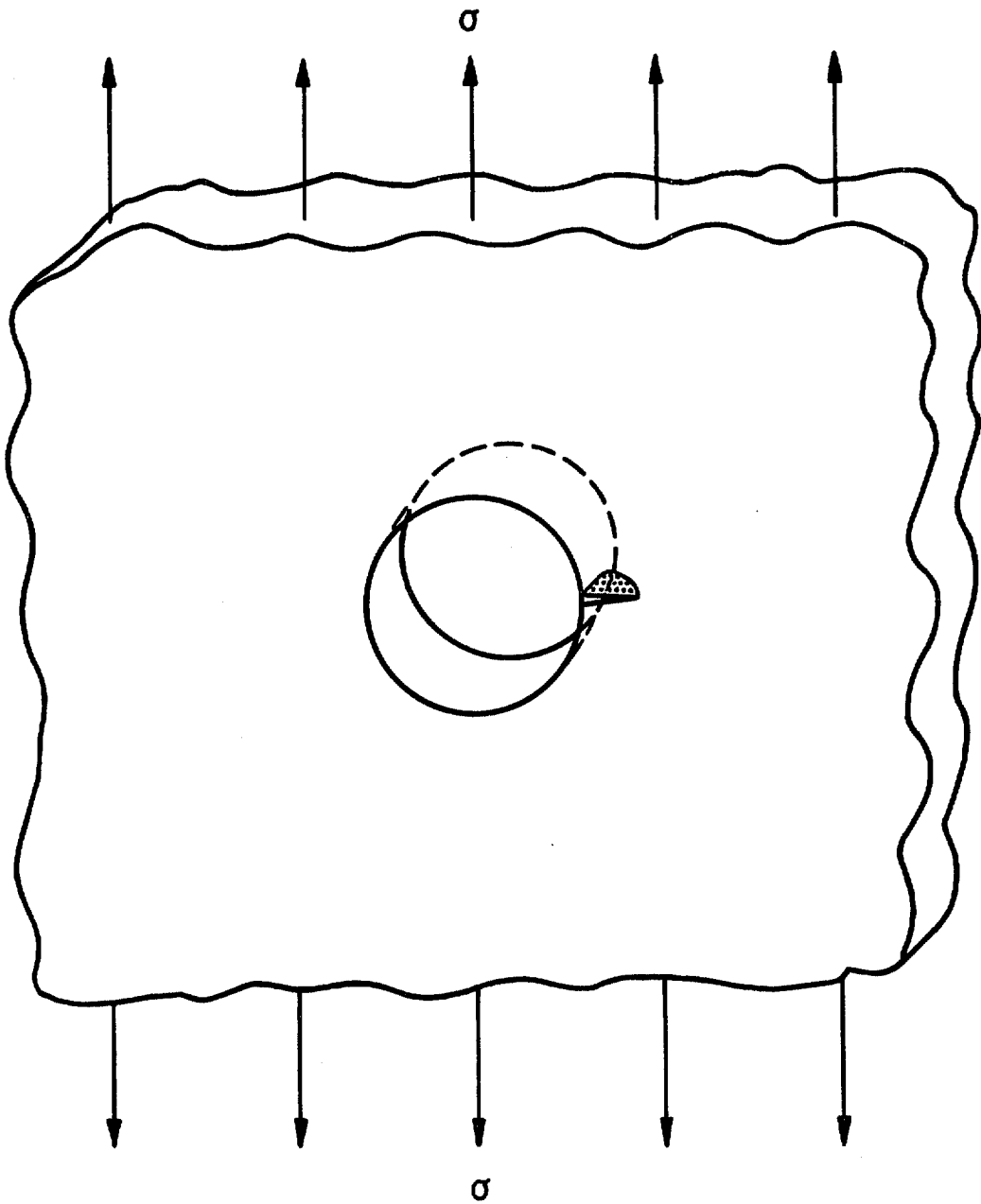
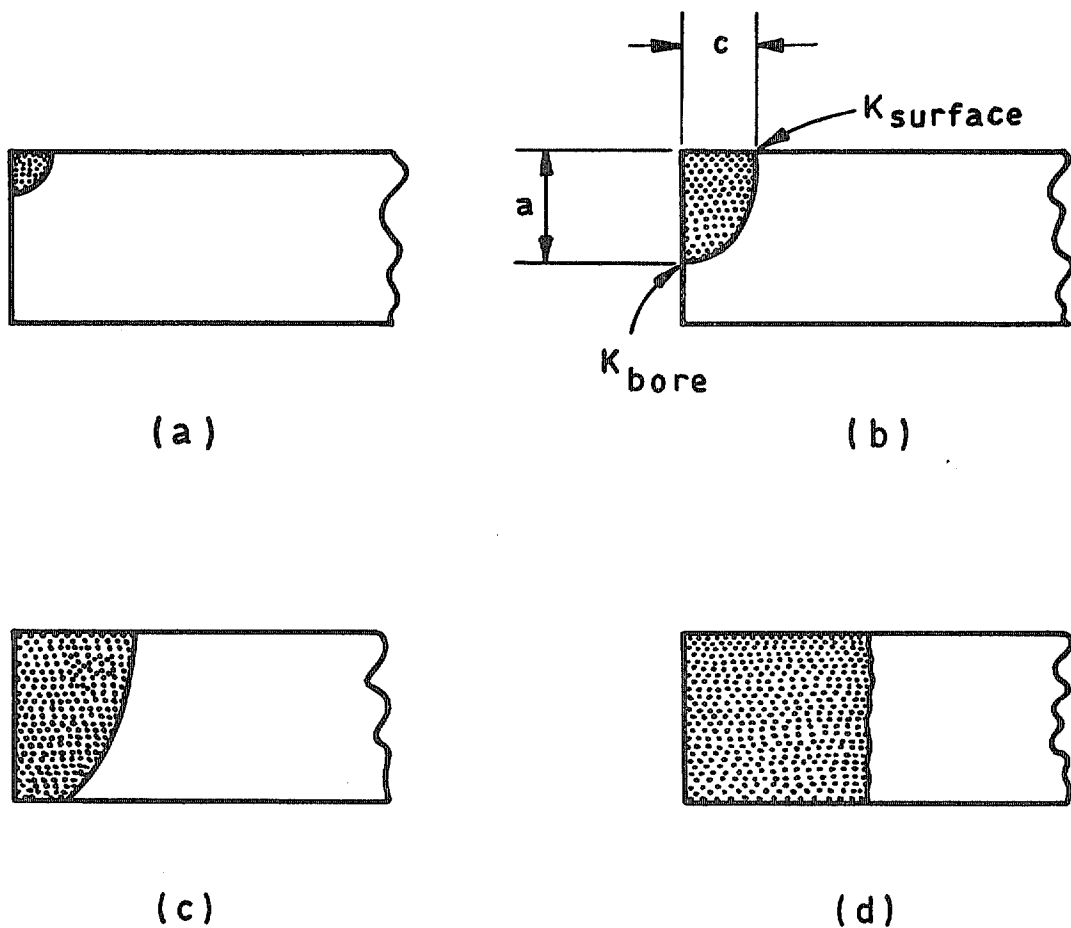


Fig 1 Corner-cracked hole in plate under uniaxial loading

Fig 2



a Length of crack down the bore of the hole

c Length of crack along surface of plate

$K_{bore}$  Stress intensity factor at intersection of crack front with bore

$K_{surface}$  Stress intensity factor at intersection of crack front with surface

Fig2 Transition of crack from quarter-circle corner-crack to through-crack

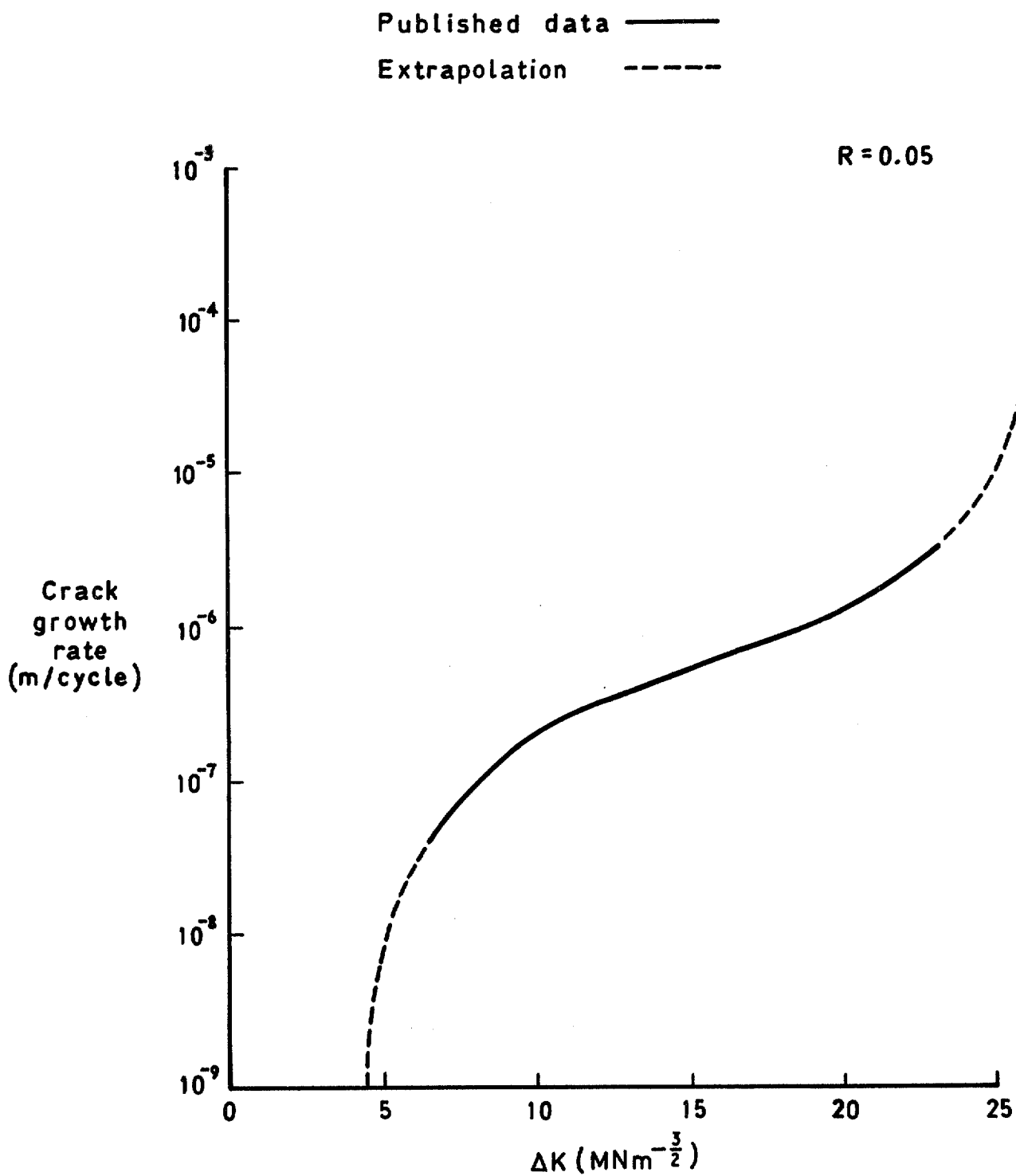


Fig 3 Extrapolation of da/dN vs  $\Delta K$  curve for DTD 5050

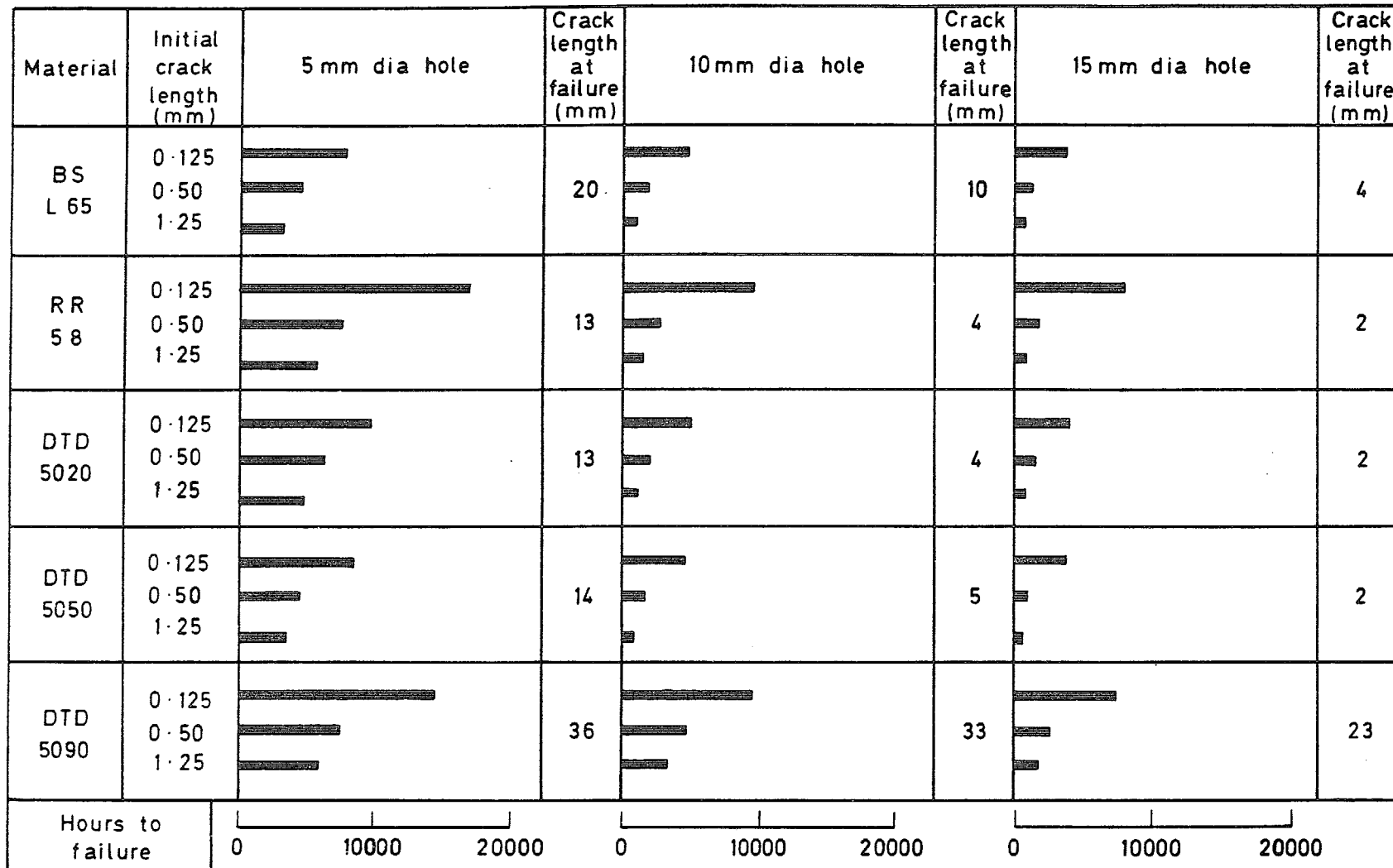


Fig 4 Summary of results. Value of stress per g =  $31 \text{ MN m}^{-2}$  ( $4500 \text{ lb in}^{-2}$ )

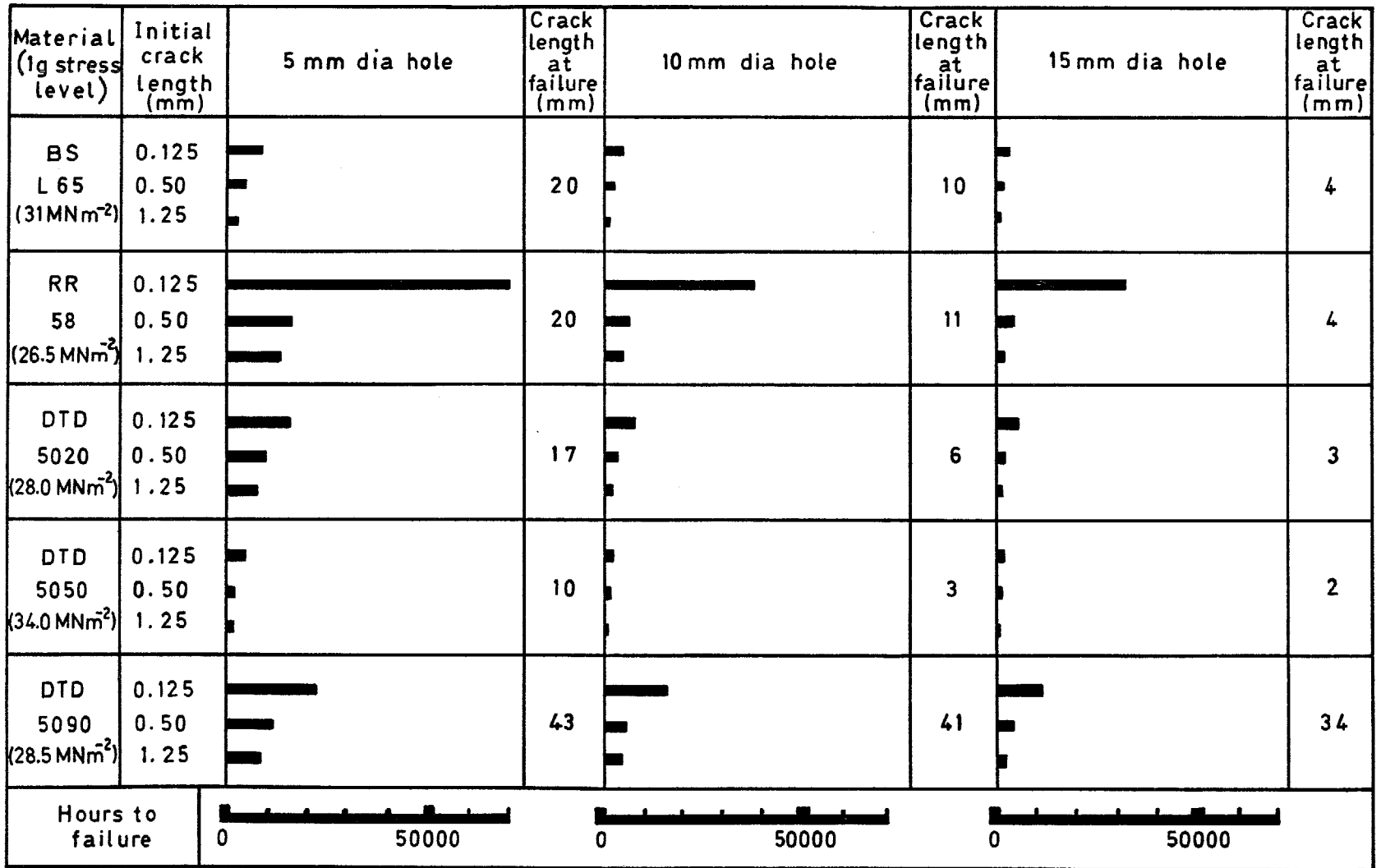


Fig 5 Summary of results. Value of stress per g = 5.9% tensile strength

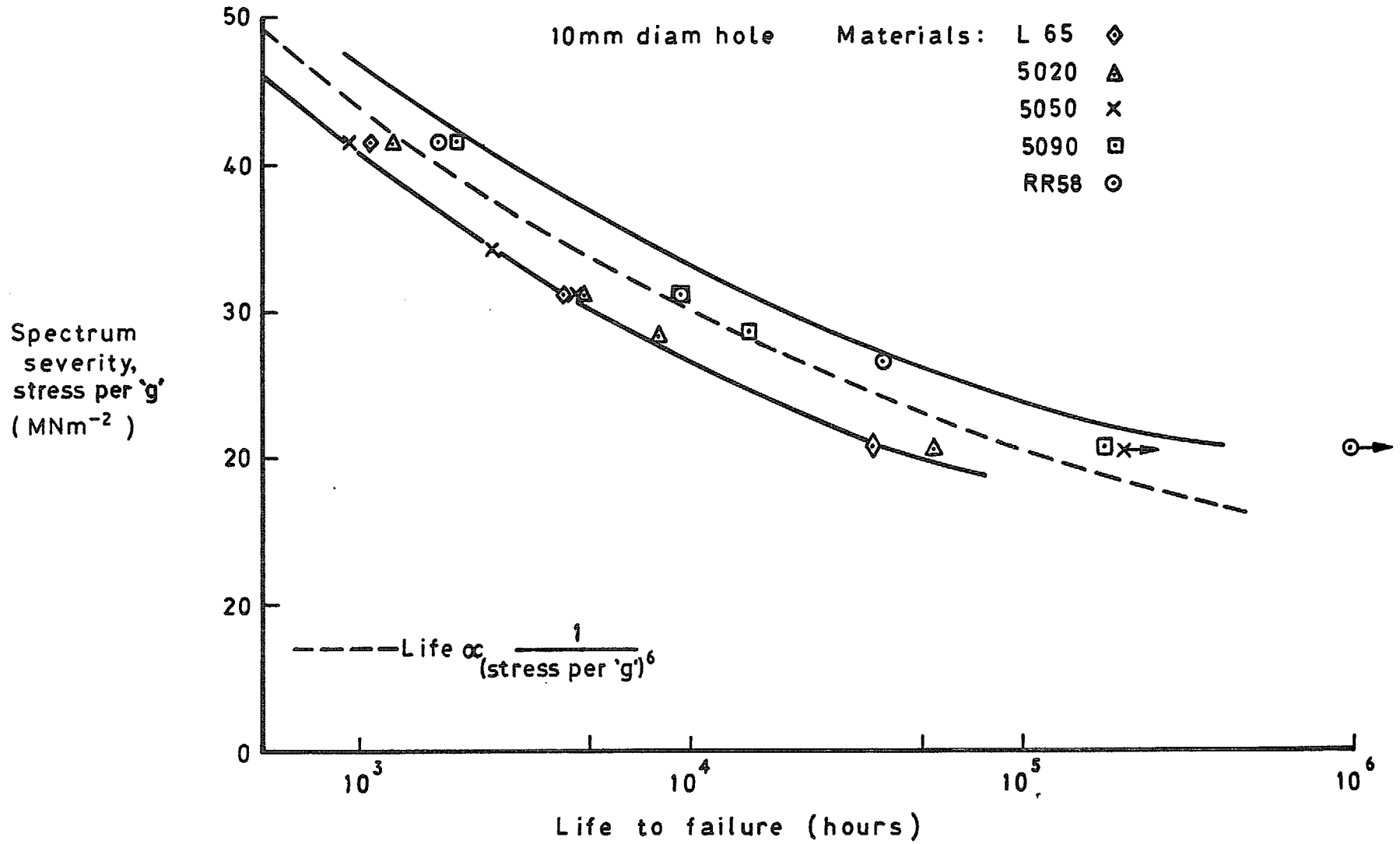


Fig 6 Effect of spectrum severity on endurance (0.125mm initial crack)

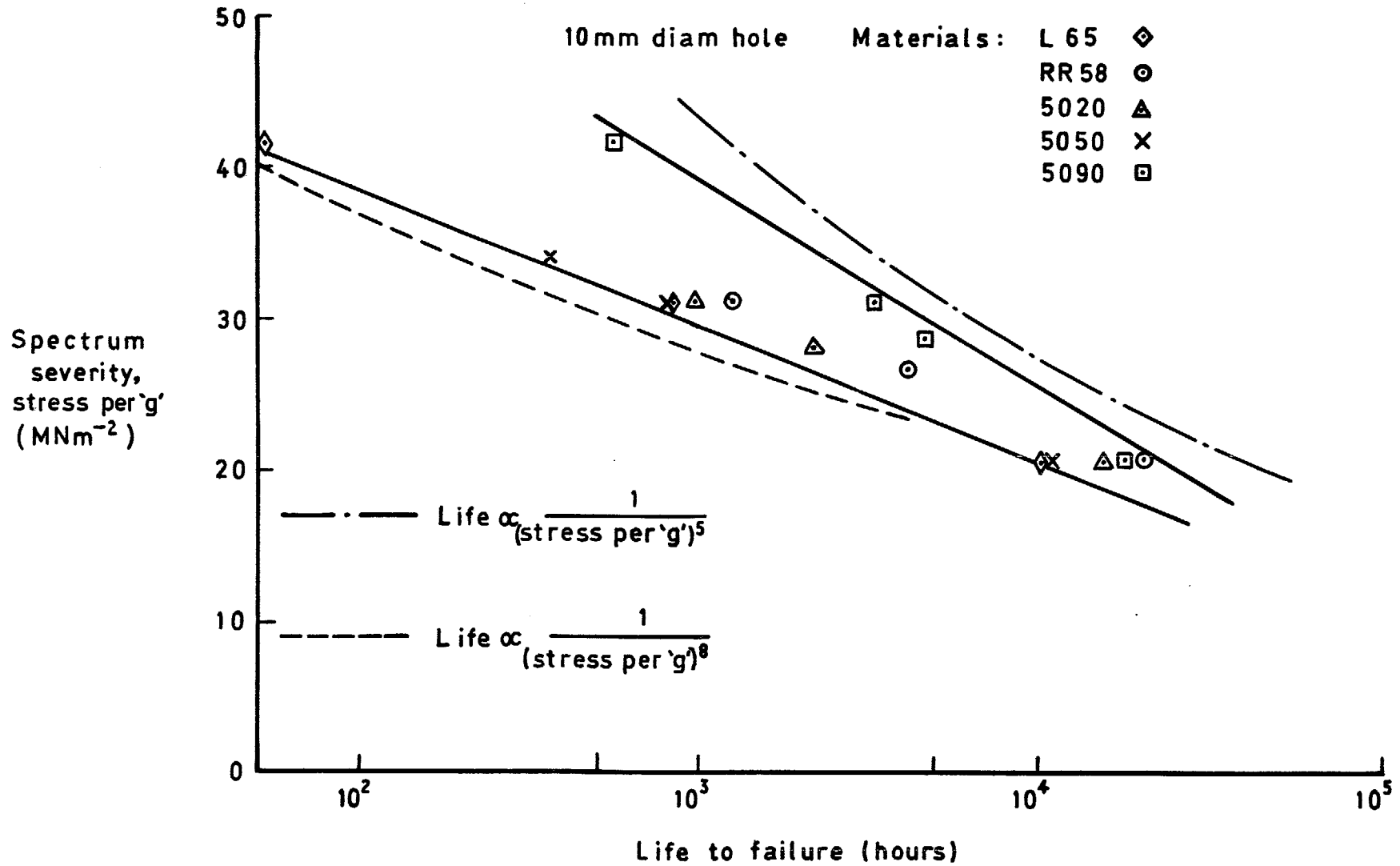
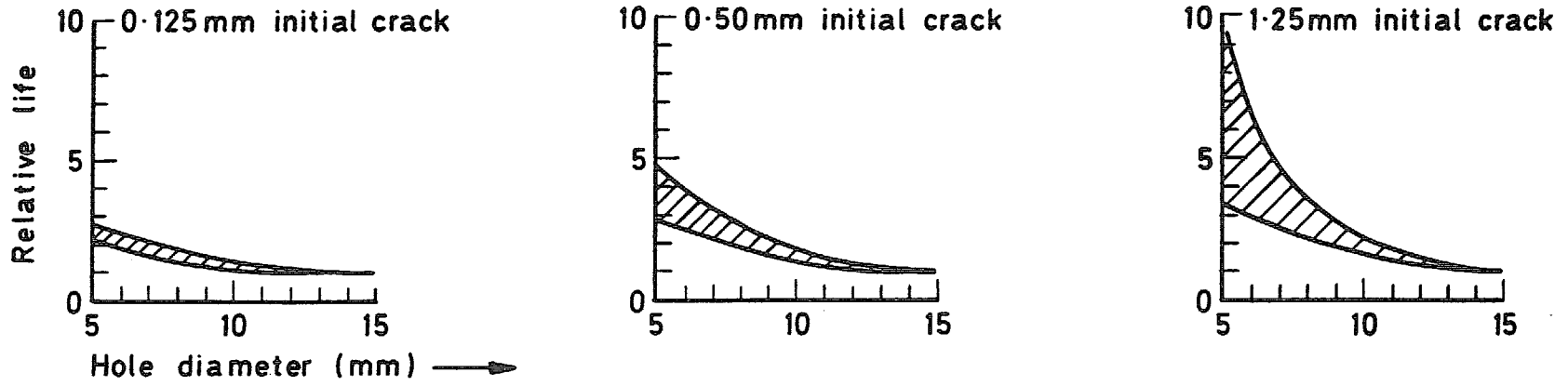
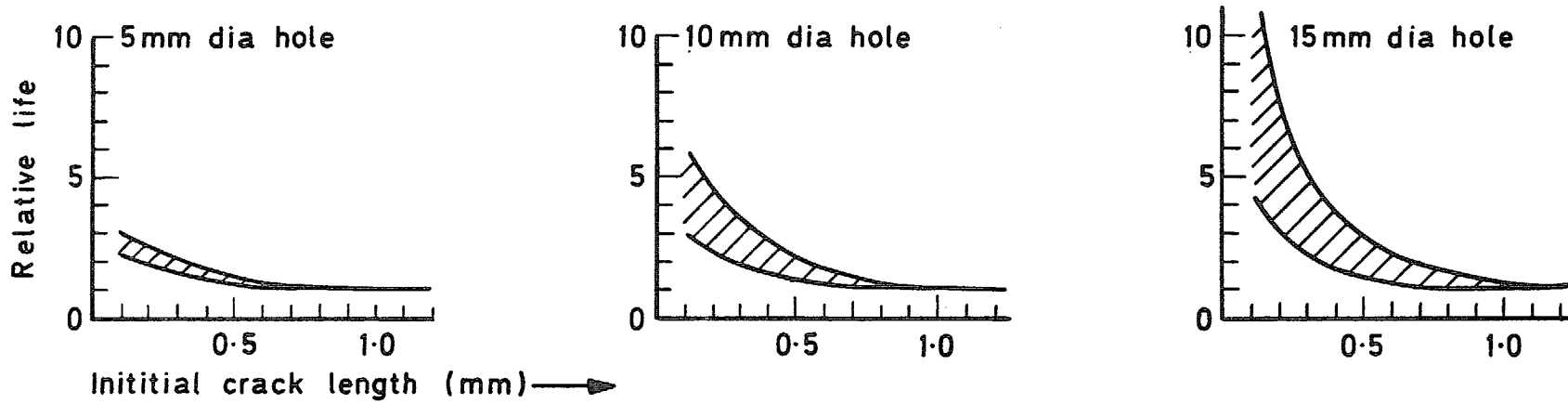


Fig 7 Effect of spectrum severity on endurance (1.25mm initial crack)



a Effect of hole diameter on life



b Effect of initial crack length on life

Fig 8 Effect of hole diameter and initial crack length on life

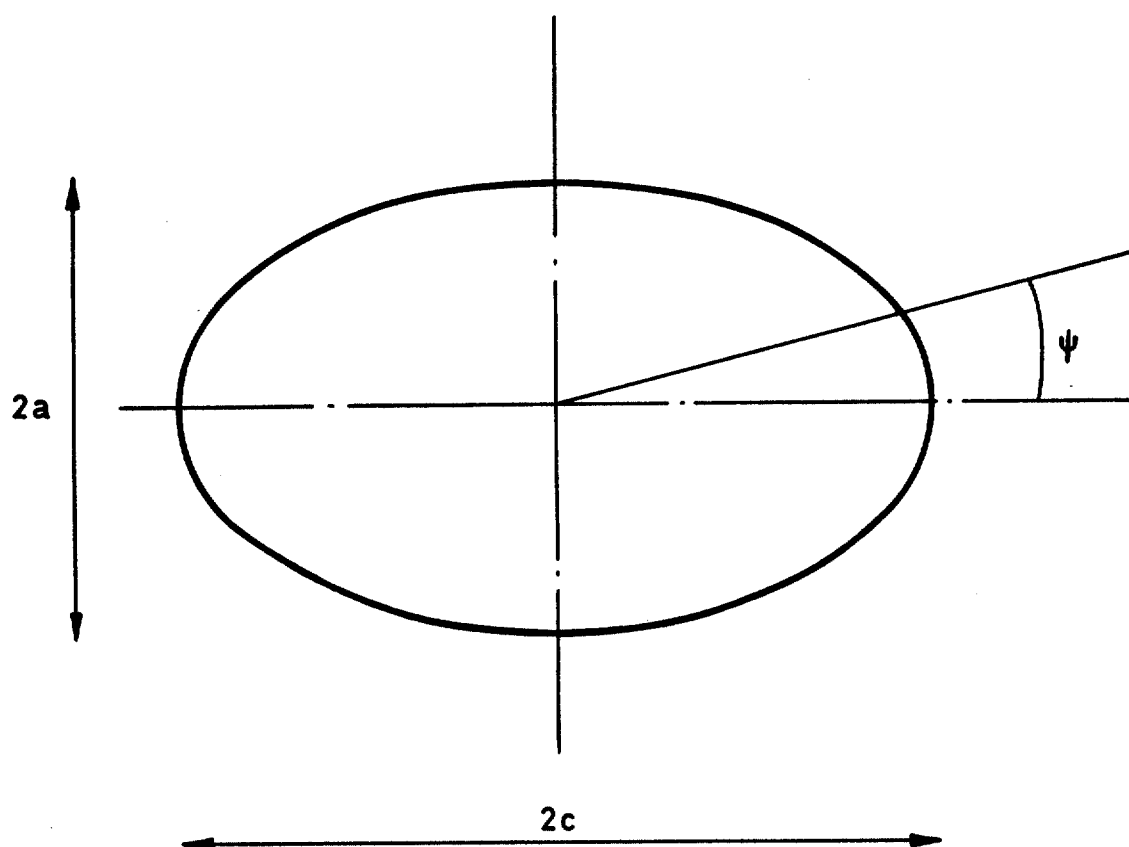


Fig 9 Notation for stress intensity factor of an embedded ellipse

R & M No. 3822

© Crown copyright

1978

Published by  
HER MAJESTY'S STATIONERY OFFICE

*Government Bookshops*

49 High Holborn, London WC1V 6HB

13a Castle Street, Edinburgh EH2 3AR

41 The Hayes, Cardiff CF1 1JW

Brazennose Street, Manchester M60 8AS

Southey House, Wine Street, Bristol BS1 2BQ

258 Broad Street, Birmingham B1 2HE

80 Chichester Street, Belfast BT1 4JY

*Government Publications are also available  
through booksellers*

HMSO

R & M No. 3822  
ISBN 0 11 471155 0